

THE MORPHOLOGY OF TYPE Ia  
SUPERNOVAE LIGHT CURVES

Mario Hamuy<sup>1,2</sup>  
M. M. Phillips<sup>1</sup>  
Nicholas B. Suntzeff<sup>1</sup>  
Robert A. Schommer<sup>1</sup>  
José Maza<sup>3,4</sup>  
R. C. Smith<sup>1,5</sup>  
P. Lira<sup>3,6</sup>  
R. Avilés<sup>1</sup>

<sup>1</sup> National Optical Astronomy Observatories\*, Cerro Tololo Inter-American Observatory, Casilla 603, La Serena, Chile

<sup>2</sup> University of Arizona, Steward Observatory, Tucson, Arizona 85721

<sup>3</sup> Departamento de Astronomía, Universidad de Chile, Casilla 36-D, Santiago, Chile

<sup>4</sup> Cátedra Presidencial de Ciencias (Chile), 1996-1997.

<sup>5</sup> University of Michigan, Department of Astronomy, Michigan 48109-1090

<sup>6</sup> Institute for Astronomy, The University of Edinburgh, Royal Observatory, Edinburgh EH9 3HJ, UK

electronic mail: mhamuy@as.arizona.edu, mphillips@noao.edu, nsuntzeff@noao.edu, rschommer@noao.edu, jmaza@das.uchile.cl, chris@astro.lsa.umich.edu, P.Lira@roe.ac.uk

Running Page Head : SNe Ia LIGHT CURVES

Address for proofs: M. M. Phillips, CTIO, Casilla 603, La Serena, Chile

Key words: photometry - supernovae -

---

\*Cerro Tololo Inter-American Observatory, National Optical Astronomy Observatories, operated by the Association of Universities for Research in Astronomy, Inc., (AURA), under cooperative agreement with the National Science Foundation.

## ABSTRACT

We present a family of six BVI template light curves for SNe Ia for days -5 and +80, based on high-quality data gathered at CTIO. These templates display a wide range of light curve morphologies, with initial decline rates of their B light curves between  $\Delta m_{15}(B)=0.87^m$  and  $1.93^m$ . We use these templates to study the general morphology of SNe Ia light curves. We find that several of the main features of the BVI templates correlate tightly with  $\Delta m_{15}(B)$ . In particular, the V light curves, which are probably a reasonably good approximation of the bolometric light curves, display an orderly progression in shapes between the most-luminous, slowest-declining events and the least-luminous, fastest-declining SNe. This supports the idea that the observed spectroscopic and photometric sequences of SNe Ia are due primarily to one parameter. Nevertheless, SNe with very similar initial decline rates do show significant differences in their light curve properties when examined in detail, suggesting the influence of one or more secondary parameters.

# 1 Introduction

The relatively small dispersion ( $\sim 0.6^m$ ) of the first Hubble diagram of Type I supernovae (SNe hereafter) constructed by Kowal (1968) revealed the potential utility of such objects as extragalactic distance indicators. Since then, considerable effort has been devoted to study the photometric properties of these objects (Leibundgut 1990, van den Bergh & Pazder 1992, Sandage & Tammann 1993). A major difficulty in these studies, however, was caused by the scarcity of photometric data. An inspection of the atlas of SNe Ia light curves (Leibundgut *et al.* 1991) reveals that most of the historical SNe possess fragmentary data and only a few observations bracket the peaks of the light curves. In order to remedy this situation in 1990 we initiated a photographic survey program, as a collaboration between the University of Chile and the Cerro Tololo Inter-American Observatory (CTIO), with the aim to discover young SNe Ia and to populate the Hubble diagram of these objects in a wide range of redshifts (Hamuy *et al.* 1993a, hereafter referred to as Paper I). In the course of 1990-93 this project yielded high-quality CCD data for  $\sim 30$  SNe Ia ( $0.01 \lesssim z \lesssim 0.1$ ) in the BVI system. Despite our efforts to discover SNe in their rising branch (by monitoring selected fields regularly twice per month), the rapid evolution of these objects often prevented their discovery until after maximum light. In fact, out of the  $\sim 30$  Calán/Tololo SNe Ia, approximately half were discovered near or at maximum light, while the other half were found within the first 15 days after maximum light (Hamuy *et al.* 1996b, hereafter referred to as paper VII).

In order to estimate peak magnitudes for those SNe with incomplete data, the technique of fitting average template light curves has been traditionally employed (eg. Leibundgut *et al.* 1991). The most widely used template has been that calculated by Leibundgut (1988) in the UBVJHK system from the best observations available at that time. However, recent studies of well-observed SNe Ia (Phillips *et al.* 1987; Phillips *et al.* 1992; Filippenko *et al.* 1992a; Filippenko *et al.* 1992b; Leibundgut *et al.* 1993; Maza *et al.* 1994, hereafter referred to as Paper II) showed that the light curves displayed by these objects are not all identical, posing an additional problem for the determination of the peak magnitudes. The need to estimate reliable peak magnitudes led us to construct a family of template curves representing the wide range of light curve morphologies of SNe Ia since, as demonstrated in Paper I, the error introduced by extrapolating a peak magnitude using an inappropriate template curve can be substantial. From the best-observed data available to us we produced six BVI template curves for different types of SNe Ia, suitable for the analysis of the Calán/Tololo database. In this paper we present these templates so that they might be available for other studies. In Sec. 2 we describe the construction procedure of the templates; in Sec. 3 we describe the properties of the templates; in Sec. 4 we perform a comparison of the individual properties of the templates and, finally, in Sec. 5 we include a short discussion of the major conclusions that can be drawn from these templates concerning the physics of SNe Ia explosions.

## 2 The construction of the templates

Since most of the photometric observations of the historical SNe were carried out with blue photographic plates, the first evidence for inhomogeneities within the Ia class was originally detected in the pg or B light curves. Specifically, a number of authors (Barbon *et al.* 1973, Pskovskii 1984, Phillips *et al.* 1987) noted that the decline rate of the B light curve during the postmaximum phase varied substantially from object to object. Recently, Phillips (1993) introduced the parameter  $\Delta m_{15}(B)$ , defined as the amount in magnitudes that the B light curve decays in the first 15 days after maximum, in order to quantify the decline rate of the B light curve. The SNe used here to construct the templates (1992bc, 1991T, 1992al, 1992A, 1992bo, 1993H, and 1991bg) were specially selected to span a range in  $\Delta m_{15}(B)$ , between  $0.87^m$  and  $1.93^m$ . With more recent data obtained at longer wavelengths, it became evident that the inhomogeneities of SNe Ia are much more pronounced in the I band than in blue light (eg. Suntzeff 1996). The selected objects are representative of the ample variety of I light curve morphologies displayed by SNe Ia. Based on these SNe, we constructed six BVI template light curves. Except for SNe 1992bo and 1993H, the light curves of each SN were sufficiently well-sampled that interpolations could be done with reasonable confidence. Since the photometry for SN 1992bo was somewhat sparser than that for other SNe, we decided to include 1993H (with a similar  $\Delta m_{15}(B)$ ) to complement the light curve of the former. In general terms, we performed the construction of the templates in the following manner:

- a) We estimated the time of maximum light in B ( $t_0^B$ ) as well as the BVI magnitudes at  $t_0^B$  of each SN by fitting a cubic spline to the data spanning days -7 to +7 (with respect to  $t_0^B$ ).
  
- b) We defined the time axis such that  $t_0^B \equiv 0$ , and then shifted each light curve individually along the magnitude axis so that  $B=V=I=0.00^m$  at  $t_0^B$ . Note that this normalization is identical to the convention adopted by Leibundgut (1988) and *preserves the original temporal separation of the BVI peaks*.
  
- c) We carried out cubic spline fits to the normalized data in the range  $-5 \leq t_0^B \leq +80$ . We performed the fits separately for various regions of the light curve, while exercising special care to guarantee the continuity of the resulting template. We interpolated values with a separation of one day in the range  $-5 \leq t_0^B \leq +32$ , every 3 days in the range  $+35 \leq t_0^B \leq +50$  and every 5 days in the range  $+55 \leq t_0^B \leq +80$ .

Next, we summarize the individual details involved in the construction of each template, presented in order of increasing values of  $\Delta m_{15}(B)$ .

## 2.1 SN 1992bc

We calculated the template for this SN from our own photometry obtained at CTIO (Paper VII). Since this SN occurred at a redshift of  $z=0.02$  we started by dividing the timescale of the observed photometry by a factor of 1.02 in order to remove the effect of time dilation. Figure 1 shows the data for SN 1992bc, duly normalized and corrected for time dilation, along with the template obtained. After calculating the template, we subtracted the K-terms for SNe Ia calculated by Hamuy *et al.* (1993b) for the corresponding redshift. Table 1 (columns 2,3,4) gives the resulting template for zero redshift. The B template is characterized by  $\Delta_{m_{15}}(B)=0.87$ .

## 2.2 SN 1991T

We calculated the template for this SN from a recent reduction of our own photometry obtained at CTIO (Lira 1995). Due to the proximity of the SN, we did not apply corrections for time dilation or K terms. Figure 2 shows the normalized data for SN 1991T along with the template obtained. Table 1 (columns 5,6,7) gives the resulting template. The B template is characterized by  $\Delta_{m_{15}}(B)=0.94$ .

## 2.3 SN 1992al

We calculated the template for this SN from our own photometry obtained at CTIO (Paper VII). Unfortunately, we could not determine the peak I magnitude for this SN because the first observation through this filter started only  $\sim 2$ -3 days after  $t_0^B$ . To get around this we adopted  $I(t_0^B=3) = 0.08^m$ , based on the average value yielded by other templates. Inspection of Table 1 shows that this is a reasonable assumption since, except for SN 1991bg (the most extreme of the templates), the normalized I magnitude at day +3 varies in a small range between  $0.06^m$  and  $0.11^m$ . After normalizing the light curves, we divided the timescale by a factor of 1.015 (since this SN occurred at a redshift of  $z=0.015$ ) in order to remove the effect of time dilation. Figure 3 shows the data for SN 1992al, duly normalized and corrected for time dilation, along with the template obtained. Shown as a dotted line in the bottom panel of this figure is an extension to the calculated template I light curve, based on an average of the remaining templates, which is our best estimate of the behavior of the I light curve at epochs  $-5 \leq t_0^B \leq +2$ . After calculating the template, we subtracted the K-terms for SNe Ia (Hamuy *et al.* 1993b) for the corresponding redshift. Table 1 (columns 8,9,10) gives the resulting template for zero redshift. The B template is characterized by  $\Delta_{m_{15}}(B)=1.11$ .

## 2.4 SN 1992A

We calculated the template for this SN from our own photometry obtained at CTIO which will be published elsewhere (Suntzeff *et al.* 1996). Due to the proximity of the SN, we did not apply corrections for time dilation or K terms. Figure 4 shows the normalized data for SN 1992A along with the template obtained. Table 1 (columns 11,12,13) lists the resulting template. The B template is characterized by  $\Delta m_{15}(B)=1.47$ .

## 2.5 SNe 1992bo and 1993H

Inspection of our photometry for SN 1992bo revealed that this object was characterized by  $\Delta m_{15}(B)\sim 1.7$  (Paper II). Although the first observations of this SN started several days before maximum light, the sampling of the I light curve around the secondary maximum did not allow us to adequately interpolate values for the construction of the template curve. The only other object with available BVI photometry and a similar decline rate is SN 1993H. Fortunately, our followup photometry for this object (Paper VII) started right at maximum light, and the sampling of the BVI light curves proved to be a good complement to the observations of SN 1992bo. An additional coincidence between this pair of SNe was their similar redshifts ( $z=0.02$  for SN 1992bo, and  $z=0.024$  for SN 1993H). We were therefore able to combine these data without worrying about redshift corrections. In doing so, we used a  $\chi^2$  minimizing procedure to determine the relative shifts in the time and magnitude scales of both objects. Once the two sets of light curves had been combined, we divided the timescale of both SNe by a factor of 1.02 to remove the effect of time dilation. Figure 5 shows the data for SNe 1992bo and 1993H, duly normalized and corrected for time dilation, along with the template obtained. After calculating the template, we subtracted the K-terms for SNe Ia calculated by Hamuy *et al.* (1993b) for the corresponding redshift. Table 1 (columns 14,15,16) gives the resulting template for zero redshift. The B light curve is characterized by  $\Delta m_{15}(B)=1.69$ .

## 2.6 SN 1991bg

We calculated the template for this SN from the photometry published by Filippenko *et al.* (1992b) and Leibundgut *et al.* (1993). These observations indicate that maximum light was observed in V. However, the first two observations obtained in B show that the SN was already in the decline phase. In order to normalize the light curve along the time axis we choose to adopt the time of the first observation in B as the time of maximum in this band. With this assumption, the time of maximum in V occurred on day +2, in agreement with other SNe Ia (see Table 1). Nevertheless, we cannot rule out the possibility that maximum light in B occurred earlier than  $t_0^B=0$ . Due to the proximity of the SN, we did not apply corrections for time dilation or K terms. Figure 6 shows the normalized data for SN 1991bg along with the

template obtained. Table 1 (columns 17,18,19) gives the resulting template. The B template is characterized by  $\Delta m_{15}(B)=1.93$ .

### 3 General properties of the templates

Figure 7 shows all of our BVI templates plotted together to illustrate the significant differences that occur within this family of light curves. Despite these differences, it is possible to identify a common pattern as well as a number of key parameters that characterize the shape of the individual templates. Among these parameters are the time and magnitude at maximum light in each band,  $t_0^k$  and  $m_0^k$ , where  $k = B, V, I$ . We can also define parameters  $\Delta m_T(k)$  which, generalizing Phillips' (1993) convention, correspond to the amount in magnitudes by which the "k" light curve decays in the first "T" days after *maximum light*. Figure 8 shows one of the BVI templates with a typical decline rate (SN 1992al) along with the graphical representation of these parameters.

The B template light curves are characterized by a rapid rise which culminates at maximum light. After maximum light the SN displays a fast-decline phase followed by a slower linear decay in luminosity. The two decline phases are separated by an *inflection* point where the curvature of the light curve changes sign. Depending on the SN, this point is located between 7 and 21 days after maximum. We call this parameter  $t_1^B$  which we define as the time when the first derivative of the B light curve reaches a maximum. Another useful time parameter is given by the intersection of the straight line that fits the exponential tail and the straight line that fits the initial decline phase of the B light curve. These two fits are shown as dotted lines in Figure 8 and we call this point the *intersection* parameter,  $t_2^B$ , which varies between day +14 and +38 depending on the SN template. This point can be considered as the onset of the exponential tail. Another useful difference of these templates is the brightness of the linear tail (relative to the peak) which we measure here with the parameter  $\Delta m_{60}(B)$ .

The V light curves have a very similar behavior to the B curves, except that the inflection is much less pronounced and that the initial postmaximum decline rate is also smaller. We introduce the parameter  $\Delta m_{20}(V)$  (using a slightly larger baseline in time than in B to compensate for the slower decline rate) in order to quantify the initial decline rate, and  $\Delta m_{60}(V)$  in order to measure the brightness of the linear tail. An interesting feature of these templates is that the time of V maximum occurs 0.5 and 2.5 days later than B maximum, in reasonable agreement with the finding of Leibundgut (1988) that  $t_0^V - t_0^B = 2.5 \pm 1.0$  days.

Except in the case of SN 1991bg, the I templates display a significantly more complex morphology than the B or V light curves. In general terms, the I templates show a primary maximum which occurs 1-2.5 days *before* B maximum; a minimum which occurs on day 11.5-19 relative to B maximum; a secondary maximum which takes place 18.5-31 days after B maximum; and a linear decline in magnitude thereafter. This secondary maximum is observed to be even

stronger in the JHK photometry of SNe Ia (Elias *et al.* 1981, 1985). Since the time of occurrence and strength of these features differ significantly within our family of templates, we use here  $(t_1^I, m_1^I)$  and  $(t_2^I, m_2^I)$  to define the time and magnitude of the minimum and the secondary maximum of the I template light curve, respectively. As opposed to the other templates, the 1991bg I template appears to be characterized by a single maximum. Unfortunately, the observations of this object started when the SN was already declining in B, so we are unable to interpret the I maximum as the primary or secondary observed in other SNe Ia. In fact, as discussed in Sec. 4, it is likely that at such fast decline rates, the primary and secondary maxima merge into a single maximum.

Table 2 lists the values of these various parameters for the different templates. We also include in this table the same parameters for two additional well-observed SNe Ia, 1990N and 1994D, which were measured from a new reduction of the CTIO photometry of SN 1990N (Lira 1995) and a preliminary reduction of photometry of SN 1994D obtained at CTIO and the Fred Whipple Observatory (Smith *et al.* 1996).

## 4 Comparison of the templates

Among the various parameters considered here, the initial postmaximum decline rate of the B light curve is the most extensively studied to date. Phillips (1993) found that the luminosities of nine nearby, well-observed SNe Ia were tightly correlated with  $\Delta m_{15}(B)$  in the sense that slow decliners proved to be the most luminous objects. The  $\sim 30$  Calán/Tololo SNe Ia provide additional support to the existence of such a relationship (Hamuy *et al.* 1996a, hereafter referred to as Paper V). In Figure 9 we show the six templates on an absolute magnitude scale set by the absolute magnitude- $\Delta m_{15}(B)$  relationship given in Paper V. Nugent *et al.* (1995) have also shown that certain optical spectral features correlate with  $\Delta m_{15}(B)$  and were able to explain these as being due principally to a correlation of the photospheric temperature with  $\Delta m_{15}(B)$ . Given the role that  $\Delta m_{15}(B)$  has played in the characterization of the intrinsic properties of SNe Ia, we choose to use it here as the central parameter in our comparison of the templates.

Figure 10 shows that the time of the *inflection* and *intersection* points of the B light curve are both well correlated with  $\Delta m_{15}(B)$ , in the sense that SNe with slower initial decline rates have a later onset of the exponential tail. Needless to say, both  $t_1^B$  and  $t_2^B$  are also very well correlated with each other. In Figure 11, we show a comparison between the initial decline rates of the B and V curves,  $\Delta m_{15}(B)$  and  $\Delta m_{20}(V)$ , which confirms the measurements given in Wells *et al.* (1994) which also indicated that the decline rates in these two colors are tightly correlated. Next, Figure 12 shows a comparison between  $\Delta m_{15}(B)$  and the relative brightness of the BVI linear tails. The top panel indicates that there is no clear relationship between  $\Delta m_{15}(B)$  and  $\Delta m_{60}(B)$ . A remarkable feature in this plot is that, while the 1992bc and 1991T templates have similar (low) decline rates, these curves differ significantly in the magnitude

drop observed between maximum light and the linear tail (see also Fig. 7). With a somewhat faster initial decline rate, the SN 1990N template displays an intermediate  $\Delta m_{60}(\text{B})$  value. Toward higher initial decline rates a regular trend is observed between the templates made from 1992al, 1994D, 1992A, and 92bo–93H. This trend is broken again by the 1991bg template which displays a relative drop at day +60 much smaller than the remaining SNe (see also Fig. 7). In contrast, Figure 12 shows that the relative brightness of the linear tails in V and I,  $\Delta m_{60}(\text{V})$  and  $\Delta m_{60}(\text{I})$  are much more tightly correlated with  $\Delta m_{15}(\text{B})$ . This suggests that  $\Delta m_{60}(\text{V})$  and  $\Delta m_{60}(\text{I})$  could be well correlated with each other and, indeed, the bottom panel of Figure 13 shows an impressive correlation between these two parameters. The upper panel of this figure shows only marginal evidence for a correlation between  $\Delta m_{60}(\text{V})$  and  $\Delta m_{60}(\text{B})$ , with SN 1991bg being the most discrepant point.

We have also compared  $\Delta m_{15}(\text{B})$  with the early-epoch properties of the I light curves. Figure 14 shows the time and magnitude of the minimum and secondary maximum plotted as a function of  $\Delta m_{15}(\text{B})$ . (Given the ambiguity in the identification of the single maximum observed for SN 1991bg, we do not include this object in this comparison.) At first sight, it is difficult to identify clear correlations in these plots. However, closer inspection reveals that most of the scatter is due to SN 1991T. Leaving aside this object, the properties of the I templates appear to be generally correlated with  $\Delta m_{15}(\text{B})$  in the sense that the strength of the minimum and secondary maximum is greater and occurs later for the slow-declining SNe (and viceversa).

In examining Figures 1-6, it becomes apparent that the second maximum in the I light curve occurs at nearly the same epoch as the prominent bend in the B light curve, which we have measured via the *intersection* parameter,  $t_2^{\text{B}}$ . This is illustrated in Figure 15, where  $t_2^{\text{I}}$  is plotted versus  $t_2^{\text{B}}$ . This correlation suggests that the primary and secondary maxima of the I light curves of the fast-declining SNe Ia probably merge into a single maximum or plateau; indeed, if we interpret the initial “peak” in the I light curve of SN 1991bg as the *secondary* maximum, the SN fits quite well on the relation plotted in Figure 15. This effect would help to explain the peculiar appearance of the H light curve of the fast-declining SN 1986G (Frogel *et al.* 1987) which exhibited a plateau at maximum light, lasting at least 20 days, rather than the familiar double-peak morphology observed in other SNe Ia (Elias *et al.* 1985).

## 5 Discussion and Conclusions

The set of templates presented in this paper were selected to be representative of the range of observed SNe Ia light curve morphologies. During the first  $\sim 100$  days following maximum light, the bolometric light curves of SNe Ia are fairly well approximated by the V light curve (e.g., see Suntzeff 1996). Focussing on the V light curves displayed in Figure 9, there appears to be an orderly progression from the most-luminous, slowly-declining events like SNe 1991T and

1992bc, to the least-luminous, fastest-declining SNe such as 92bo/93H and 1991bg. The strong correlations between  $\Delta m_{15}(B)$  and the two V light curve decline rate parameters  $\Delta m_{20}(V)$  and  $\Delta m_{60}(V)$  (see Figures 11 & 12) strengthens the impression that the light curve shapes are governed primarily by a single parameter, consistent with the suggestion by Nugent *et al.* (1995) that the observed spectroscopic and photometric sequences of SNe Ia are due primarily to one parameter. These authors concluded that the parameter was most likely the mass of radioactive  $^{56}\text{Ni}$  produced in the explosion. Assuming that the physical conditions in the ejecta of the different SNe during the final exponential decline phase are similar, the different luminosities during this phase could be interpreted as reflecting differing  $^{56}\text{Ni}$  masses. Pinto & Eastman (1996) have argued that the relative factor is actually the mass of the progenitor white dwarf star, with masses in the range 0.5-1.4  $M_{\odot}$  required to explain the range of observed luminosities and decline rates.

Nevertheless, a detailed comparison of the templates of the two slowest-declining, most-luminous SNe Ia, 1992bc and 1991T, shows that one or more additional parameters probably influence the light curve shapes. This is seen most clearly by comparing the B and I light curves of these two events (see Figure 7). Although the initial decline rates of 1992bc and 1991T as measured by both  $\Delta m_{15}(B)$  and  $\Delta m_{20}(V)$  are very similar, this phase lasts significantly longer in 1992bc ( $t_2^B$  occurred 6 days later for 1992bc than it did for 1991T). This, in turn leads to the quite different values of  $\Delta m_{60}(B)$  observed for these two SNe. We note that while the premaximum spectrum of SN 1992bc was very similar to other “typical” SNe Ia (Hamuy *et al.*, in preparation), SN 1991T was an abnormal object with a variety of premaximum spectroscopic peculiarities (Filippenko *et al.* 1992a; Phillips *et al.* 1992). Another case in point is SN 1990N, which displayed decline rates in B and V that were essentially identical to those of SN 1992al, but whose values of  $\Delta m_{60}(B)$ ,  $\Delta m_{60}(V)$ , and  $\Delta m_{60}(I)$  were more similar to those of the slower-declining SN 1991T. These small differences could be due to variations in parameters such as the explosion energy/mechanism and/or the distribution of  $^{56}\text{Ni}$  in the ejecta.

Finally, we consider the fastest-declining event in our sample, SN 1991bg. From Figure 7, one might conclude that this SN does not “fit in” well with the other SNe Ia since the final exponential tail of the B light curve sets in very early, causing the template to cross the other template curves. This same property is responsible for the discrepant position of 1991bg in the top panels of Figures 12 and 13. However, in Figure 9 which is a more physically-meaningful plot of the templates, 1991bg does not appear to be nearly so discordant. Note in particular that the exponential decline phase of the B light curve does *not* cross the other template curves. The low luminosity of this SN in the B band and its unusually red B-V color at maximum (Filippenko *et al.* 1992b; Leibundgut *et al.* 1993) were almost certainly due to a lower than “normal” (Nugent *et al.* 1995) effective temperature. As mentioned earlier, the bolometric light curves of all of these SNe are probably closest to the V light curves, and the V light curve of 1991bg appears to be a fairly smooth extrapolation of the other template curves (see Figures 7 and 9). Hence, we conclude that the VRI light curve shapes of SN 1991bg are consistent with the idea that a single major parameter can explain the major characteristics of the observed sequence of light curve morphologies for SNe Ia.

## Acknowledgments

This paper has been possible thanks to grant 92/0312 from Fondo Nacional de Ciencias y Tecnología (FONDECYT-Chile). MH acknowledges support provided for this work by the National Science Foundation through grant number GF-1002-96 from the Association of Universities for Research in Astronomy, Inc., under NSF Cooperative Agreement No. AST-8947990 and from Fundación Andes under project C-12984. JM and MH acknowledge support by Cátedra Presidencial de Ciencias 1996-1997.

## References

- Barbon, R., Ciatti, F., & Rosino, L. 1973, *A&AS*, 25, 241
- Elias, J.H., Frogel, J.A., Hackwell, J.A., & Persson, S.E. 1981, *ApJ*, 251, L13
- Elias, J.H., Matthews, K., Neugebauer, G., & Persson, S.E. 1985, *ApJ*, 296, 379
- Filippenko, A.V., *et al.* 1992a, *ApJ*, 384, L15
- Filippenko, A.V., *et al.* 1992b, *AJ*, 104, 1543
- Frogel, J.A., Gregory, B., Kawara, K., Laney, D., Phillips, M.M., Terndrup, D., Vrba, F., & Whitford, A.E. 1987, *ApJ*, 315, L129
- Hamuy, M., *et al.* 1993a, *AJ*, 106, 2392 (Paper I)
- Hamuy, M., Phillips, M.M., Wells, L.A., & Maza, J. 1993b, *PASP*, 105, 787
- Hamuy, M., Phillips, M.M., Schommer, R.A., Suntzeff, N.B., Maza, J., & Avilés, R. 1996a, *AJ*, this volume (Paper V)
- Hamuy, M., *et al.* 1996b, *AJ*, this volume (Paper VII)
- Kowal, C.T. 1968, *AJ*, 73, 1021
- Leibundgut, B. 1988, Ph.D. thesis, University of Basel
- Leibundgut, B. 1990, in *Supernovae*, edited by S.E. Woosley (Springer, Berlin), p. 751
- Leibundgut, B., Tammann, G.A., Cadonau, R., & Cerrito, D. 1991, *A&AS*, 89, 537
- Leibundgut, B., *et al.* 1993, *AJ*, 105, 301
- Lira, P. 1995, MS Thesis, Universidad de Chile
- Maza, J., Hamuy, M., Phillips, M.M., Suntzeff, N.B., & Avilés, R. 1994, *ApJ*, 424, L107 (Paper II)
- Nugent, P., Phillips, M., Baron, E., Branch, D., & Hauschildt, P. 1995, *ApJ*, 455, L147
- Phillips, M.M., *et al.* 1987, *PASP*, 99, 592
- Phillips, M.M., Wells, L.A., Suntzeff, N.B., Hamuy, M., Leibundgut, B., Kirshner, R.P., &

Foltz, C.B. 1992, AJ, 103, 1632

Phillips, M.M. 1993, ApJ, 413, L105

Pinto, P.A., & Eastman, R.G. 1996, in preparation

Pskovskii, Y.P. 1984, SvA, 28, 658

Sandage, A., & Tammann, G.A. 1993, ApJ, 415, 1

Smith, R.C., *et al.* 1996, in preparation

Suntzeff, N.B. 1996, in *Supernovae and Supernova Remnants*, IAU Colloquium 145, ed. R. McCray (Cambridge University Press, Cambridge), in press

Suntzeff, N.B., *et al.* 1996, in preparation

van den Bergh, S., & Pazder, J. 1992, ApJ, 390, 34

Wells, L.A., *et al.* 1994, AJ, 108, 2233

## Figure Captions

Figure 1. The B (top), V (middle), and I (bottom) light curves of SN 1992bc, duly normalized and corrected for time dilation, along with the calculated template. The B template is characterized by  $\Delta m_{15}(B)=0.87^m$ .

Figure 2. The B (top), V (middle), and I (bottom) light curves of SN 1991T, duly normalized, along with the calculated template. The B template is characterized by  $\Delta m_{15}(B)=0.94^m$ .

Figure 3. The B (top), V (middle), and I (bottom) light curves of SN 1992al, duly normalized and corrected for time dilation, along with the calculated template. Shown as dotted lines in the bottom panel is an extension to the calculated template I light curve, based on an average of the remaining templates. The B template is characterized by  $\Delta m_{15}(B)=1.11^m$ .

Figure 4. The B (top), V (middle), and I (bottom) light curves of SN 1992A, duly normalized, along with the calculated template. The B template is characterized by  $\Delta m_{15}(B)=1.47^m$ .

Figure 5. The B (top), V (middle), and I (bottom) light curves of SNe 1992bo (open circles) and 1993H (crosses), duly normalized and corrected for time dilation, along with the calculated template. The B template is characterized by  $\Delta m_{15}(B)=1.69^m$ .

Figure 6. The B (top), V (middle), and I (bottom) light curves of SN 1991bg, duly normalized, along with the calculated template. The B template is characterized by  $\Delta m_{15}(B)=1.93^m$ .

Figure 7. The comparison of the six template B (top), V (middle), and I (bottom) light curves of SNe Ia, all normalized such that  $m^k(t_0^B)=0$  in all three bands ( $k=B,V,I$ ).

Figure 8. The template B (top), V (middle), and I (bottom) light curves of SN 1992al. Also shown are the graphical representations of the key parameters defined here in order to characterize the shape of the individual templates.

Figure 9. The six templates B (top), V (middle), and I (bottom) light curves of SNe Ia, on the absolute magnitude scale set by the peak luminosity- $\Delta m_{15}(B)$  relationship of Paper V. The peak absolute magnitudes for the five templates with  $0.87 \leq \Delta m_{15}(B) \leq 1.69$  were calculated using the “low-extinction” fits given in Table 3 of Paper V. The SN 1991bg template is plotted at the peak absolute magnitudes given in Table 1 of Paper V for the fast-declining event SN 1992K.

Figure 10. (top) The *inflection* point of the B light curve,  $t_1^B$ , as a function of  $\Delta m_{15}(B)$ . (bottom) The *intersection* point of the B light curve,  $t_2^B$ , as a function of  $\Delta m_{15}(B)$ .

Figure 11. The initial decline rate of the V template light curves,  $\Delta m_{20}(V)$ , plotted as a function of the initial decline rate of the B template light curves,  $\Delta m_{15}(B)$ .

Figure 12. Comparison of the initial decline rate of the B light curve,  $\Delta m_{15}(B)$ , and the brightness of the linear tail (relative to maximum light) of the B (top), V (middle), and I (bottom) template light curves.

Figure 13. (top) The brightness of the linear tail (relative to maximum light) of the B template light curves, plotted as a function of the brightness of the linear tail (relative to maximum light) of the V template light curves. (bottom) The same plot for the I template curves.

Figure 14. (top) The time and magnitude of the minimum of the I template light curves, plotted as a function of  $\Delta m_{15}(B)$ . (bottom) The time and magnitude of the secondary maximum of the I template light curves, plotted as a function of  $\Delta m_{15}(B)$ .

Figure 15. The time of the secondary maximum of the I template light curves,  $t_2^I$ , plotted as a function of the time of occurrence of the bend in the B light curves as measured by the *intersection* parameter,  $t_2^B$ .

Table 1. Templates for Type Ia Supernovae

(1)	(2)	(3)	(4)	(5)	(6)	(7)	(8)	(9)	(10)	(11)	(12)	(13)	(14)	(15)	(16)	(17)	(18)	(19)
$t-t_0^B$ days	B mag	1992bc V mag	I mag	B mag	1991T V mag	I mag	B mag	1992al V mag	I mag	B mag	1992A V mag	I mag	B mag	92bo-93H V mag	I mag	B mag	1991bg V mag	I mag
-5.0	0.25	0.27	0.07	0.14	0.22	0.09	0.20	0.23	0.11	0.30	0.31	0.06	0.34	0.34	0.10	....	....	....
-4.0	0.16	0.18	0.03	0.09	0.15	0.05	0.13	0.15	0.05	0.19	0.21	-0.02	0.21	0.23	0.03	....	....	....
-3.0	0.10	0.11	-0.01	0.05	0.10	0.02	0.07	0.09	0.00	0.10	0.14	-0.05	0.12	0.14	-0.01	....	....	....
-2.0	0.06	0.06	-0.02	0.02	0.06	-0.00	0.03	0.04	-0.01	0.04	0.08	-0.05	0.06	0.08	-0.02	....	....	....
-1.0	0.02	0.03	-0.02	0.00	0.02	-0.00	0.00	0.01	-0.01	0.01	0.03	-0.03	0.01	0.04	-0.02	....	....	....
0.0	0.00	0.00	0.00	0.00	0.00	0.00	0.00	0.00	0.00	0.00	0.00	0.00	0.00	0.00	0.00	0.00	0.00	0.00
1.0	0.01	0.00	0.02	0.00	-0.01	0.01	0.01	0.00	0.02	0.03	-0.02	0.02	0.01	0.00	0.04	0.05	-0.04	-0.04
2.0	0.02	0.01	0.06	0.02	-0.02	0.03	0.03	0.01	0.05	0.07	-0.03	0.04	0.04	0.01	0.05	0.10	-0.05	-0.07
3.0	0.04	0.03	0.11	0.05	-0.02	0.06	0.05	0.02	0.08	0.14	-0.02	0.06	0.10	0.03	0.09	0.19	-0.04	-0.09
4.0	0.08	0.05	0.15	0.08	-0.01	0.10	0.10	0.04	0.12	0.21	0.01	0.10	0.17	0.07	0.14	0.31	0.00	-0.10
5.0	0.13	0.08	0.20	0.13	0.01	0.14	0.15	0.06	0.16	0.29	0.04	0.17	0.26	0.10	0.20	0.46	0.07	-0.09
6.0	0.18	0.12	0.26	0.18	0.03	0.19	0.22	0.09	0.21	0.38	0.09	0.25	0.37	0.15	0.25	0.65	0.15	-0.07
7.0	0.24	0.16	0.33	0.25	0.07	0.26	0.29	0.13	0.25	0.47	0.15	0.33	0.48	0.21	0.31	0.85	0.26	-0.04
8.0	0.31	0.22	0.39	0.32	0.10	0.31	0.38	0.18	0.32	0.57	0.22	0.42	0.62	0.27	0.36	1.06	0.37	-0.01
9.0	0.37	0.27	0.46	0.39	0.14	0.35	0.46	0.23	0.43	0.68	0.30	0.49	0.75	0.34	0.41	1.25	0.50	0.04
10.0	0.45	0.31	0.53	0.47	0.18	0.38	0.57	0.28	0.51	0.79	0.38	0.53	0.91	0.40	0.45	1.42	0.64	0.09
11.0	0.53	0.37	0.58	0.56	0.23	0.39	0.67	0.34	0.57	0.92	0.45	0.54	1.06	0.47	0.47	1.57	0.76	0.16
12.0	0.61	0.42	0.63	0.64	0.28	0.40	0.78	0.38	0.61	1.05	0.52	0.54	1.24	0.55	0.49	1.68	0.89	0.22
13.0	0.70	0.48	0.68	0.74	0.34	0.41	0.89	0.44	0.64	1.19	0.59	0.52	1.40	0.62	0.49	1.79	1.01	0.29
14.0	0.78	0.53	0.73	0.84	0.39	0.40	1.01	0.51	0.65	1.33	0.65	0.50	1.55	0.69	0.49	1.87	1.12	0.36
15.0	0.87	0.58	0.75	0.94	0.45	0.39	1.11	0.58	0.66	1.47	0.71	0.46	1.69	0.77	0.47	1.93	1.21	0.44
16.0	0.96	0.64	0.78	1.05	0.51	0.38	1.23	0.64	0.65	1.62	0.77	0.42	1.84	0.87	0.45	1.98	1.30	0.52
17.0	1.05	0.69	0.79	1.15	0.56	0.37	1.34	0.70	0.64	1.75	0.82	0.38	1.96	0.96	0.44	2.02	1.37	0.60
18.0	1.14	0.74	0.81	1.26	0.62	0.37	1.47	0.76	0.62	1.88	0.88	0.35	2.09	1.04	0.43	2.05	1.44	0.69
19.0	1.24	0.78	0.82	1.36	0.67	0.36	1.58	0.83	0.60	2.01	0.94	0.33	2.22	1.11	0.43	2.09	1.50	0.78
20.0	1.35	0.82	0.81	1.47	0.72	0.35	1.69	0.89	0.58	2.12	1.01	0.32	2.32	1.21	0.44	2.14	1.55	0.85
21.0	1.45	0.87	0.81	1.58	0.77	0.34	1.81	0.94	0.56	2.23	1.09	0.32	2.42	1.31	0.46	2.18	1.59	0.92
22.0	1.55	0.91	0.79	1.69	0.83	0.34	1.92	1.00	0.54	2.34	1.20	0.34	2.52	1.37	0.50	2.22	1.63	0.98
23.0	1.65	0.95	0.78	1.80	0.88	0.34	2.02	1.07	0.53	2.44	1.29	0.37	2.61	1.45	0.56	2.27	1.67	1.04
24.0	1.74	1.00	0.76	1.90	0.93	0.34	2.12	1.13	0.51	2.54	1.37	0.42	2.69	1.51	0.62	2.30	1.72	1.11
25.0	1.83	1.06	0.75	1.99	0.99	0.35	2.22	1.19	0.50	2.63	1.46	0.49	2.75	1.58	0.70	2.33	1.77	1.17
26.0	1.92	1.10	0.73	2.07	1.04	0.35	2.32	1.25	0.50	2.73	1.54	0.57	2.82	1.64	0.80	2.36	1.82	1.23
27.0	2.02	1.16	0.72	2.14	1.09	0.36	2.40	1.30	0.50	2.81	1.61	0.65	2.88	1.70	0.89	2.38	1.86	1.29
28.0	2.10	1.21	0.71	2.21	1.14	0.38	2.48	1.36	0.51	2.89	1.68	0.74	2.92	1.76	0.94	2.41	1.92	1.35
29.0	2.19	1.27	0.70	2.27	1.19	0.40	2.55	1.41	0.53	2.94	1.74	0.83	2.96	1.82	1.03	2.44	1.97	1.41
30.0	2.27	1.30	0.69	2.33	1.24	0.42	2.63	1.46	0.55	3.00	1.80	0.93	2.98	1.86	1.10	2.46	2.02	1.47
31.0	2.34	1.36	0.69	2.38	1.29	0.45	2.69	1.50	0.58	3.03	1.86	1.01	3.03	1.92	1.18	2.49	2.07	1.53
32.0	2.42	1.41	0.69	2.43	1.33	0.48	2.74	1.55	0.62	3.06	1.91	1.09	3.07	1.97	1.25	2.52	2.12	1.59
35.0	2.62	1.56	0.74	2.56	1.47	0.60	2.90	1.70	0.77	3.14	2.05	1.27	3.16	2.12	1.45	2.60	2.26	1.76
38.0	2.77	1.70	0.82	2.66	1.59	0.75	3.02	1.83	0.93	3.22	2.16	1.43	3.24	2.25	1.63	2.68	2.40	1.93
41.0	2.91	1.84	0.98	2.76	1.71	0.90	3.11	1.95	1.11	3.29	2.26	1.58	3.32	2.38	1.82	2.76	2.54	2.09
44.0	3.03	1.98	1.15	2.84	1.83	1.08	3.19	2.07	1.28	3.36	2.35	1.73	3.39	2.49	1.97	2.84	2.66	2.25
47.0	3.12	2.09	1.36	2.90	1.93	1.26	3.27	2.18	1.46	3.41	2.43	1.88	3.45	2.59	2.14	2.90	2.77	2.40
50.0	3.20	2.21	1.56	2.96	2.04	1.43	3.34	2.28	1.64	3.45	2.51	2.03	3.50	2.68	2.29	2.98	2.88	2.55
55.0	3.29	2.39	1.87	3.05	2.21	1.69	3.39	2.45	1.87	3.51	2.65	2.27	3.58	2.83	2.54	3.09	3.04	2.78
60.0	3.36	2.54	2.09	3.12	2.37	1.92	3.47	2.59	2.09	3.56	2.78	2.50	3.64	2.96	2.76	3.19	3.19	3.00
65.0	3.42	2.69	2.32	3.19	2.51	2.11	3.53	2.74	2.30	3.61	2.92	2.73	3.71	3.10	3.00	3.30	3.33	3.22
70.0	3.48	2.83	2.53	3.29	2.64	2.32	3.60	2.87	2.51	3.66	3.06	2.94	3.77	3.24	3.21	3.40	3.47	3.41
75.0	3.55	2.96	2.74	3.38	2.75	2.54	3.66	2.98	2.72	3.72	3.20	3.15	3.86	3.39	3.44	3.49	3.62	3.59
80.0	3.62	3.08	2.94	3.46	2.86	2.73	3.73	3.11	2.92	3.80	3.34	3.35	3.96	3.55	3.68	3.58	3.76	3.76

Table 2. Parameters for Template Light Curves

SN	$\Delta m_{15}(B)$ mag	$t_1^B$ days	$t_2^B$ days	$\Delta m_{60}(B)$ mag	$t_0^V$ days	$m_0^V$ mag	$\Delta m_{20}(V)$ mag	$\Delta m_{60}(V)$ mag	$t_0^I$ days	$m_0^I$ mag	$t_1^I$ days	$m_1^I$ mag	$t_2^I$ days	$m_2^I$ mag	$\Delta m_{60}(I)$ mag
92bc	0.87	20.6	38.0	3.36	0.5	0.00	0.85	2.56	-1.5	-0.02	19.0	0.82	31.0	0.69	2.04
91T	0.94	19.0	32.0	3.12	2.5	-0.02	0.88	2.46	-1.0	0.00	13.0	0.41	22.5	0.34	1.88
92al	1.11	16.9	33.0	3.47	0.5	0.00	0.92	2.61	-1.5	-0.01	15.0	0.66	26.0	0.50	2.04
92A	1.47	14.1	28.5	3.56	2.0	-0.03	1.23	2.87	-2.5	-0.05	11.5	0.54	20.5	0.32	2.44
92bo-93H	1.69	11.6	25.0	3.64	0.5	0.00	1.26	2.97	-1.5	-0.02	13.0	0.49	18.5	0.43	2.71
91bg	1.93	7.0	14.0	3.19	2.0	-0.05	1.68	3.30	4.0?	-0.10?	...	...	4.0?	-0.10	3.28
90N	1.07	15.8	34.0	3.24	2.5	-0.01	0.90	2.42	-2.1	-0.02	16.5	0.58	...	...	1.72
94D	1.32	15.6	28.5	3.54	1.0	0.00	1.14	2.81	-2.7	-0.04	11.9	0.68	20.7	0.44	2.51

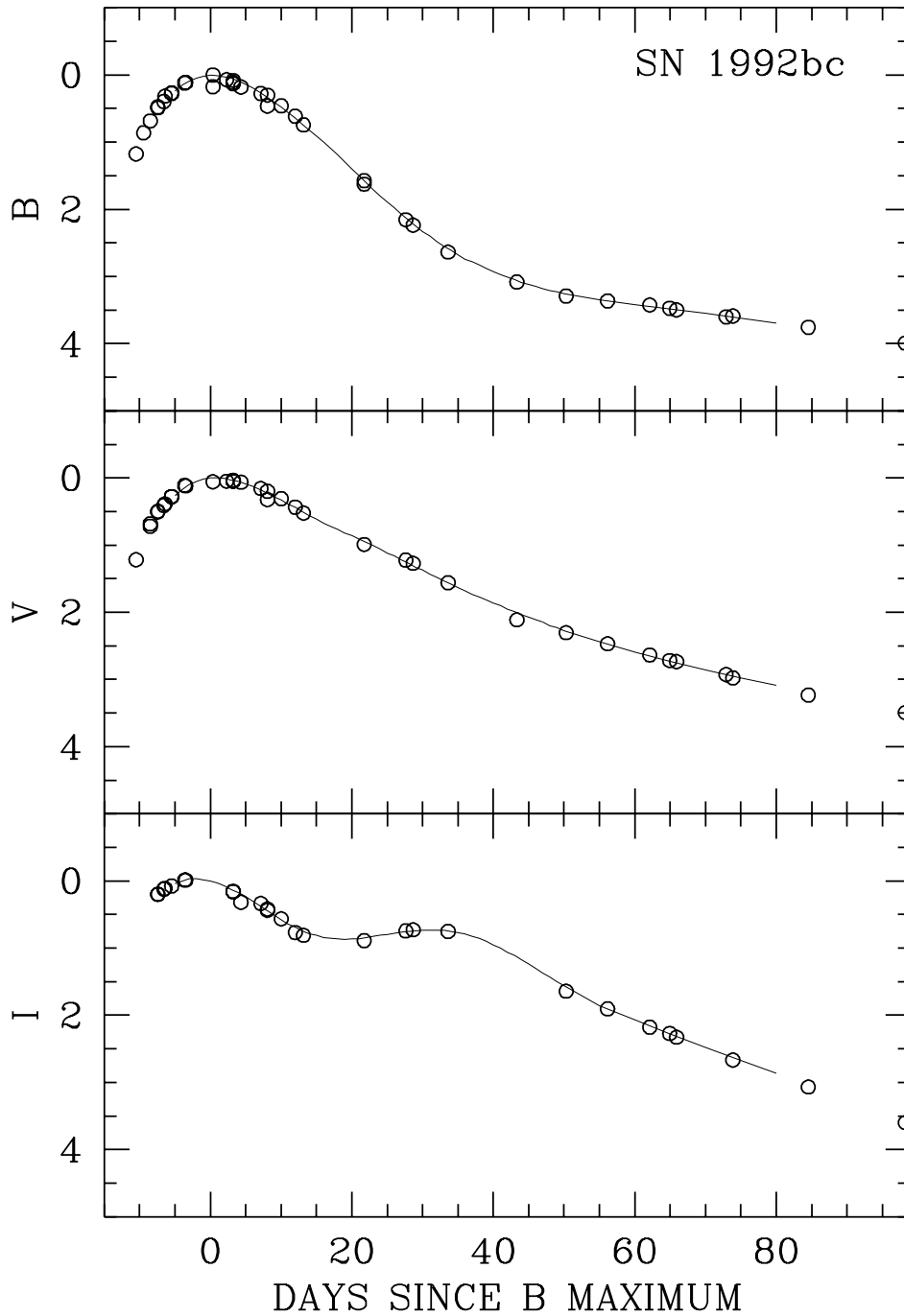


Figure 1: The B (top), V (middle), and I (bottom) light curves of SN 1992bc, duly normalized and corrected for time dilation, along with the calculated template. The B template is characterized by  $\Delta m_{15}(B)=0.87^m$ .

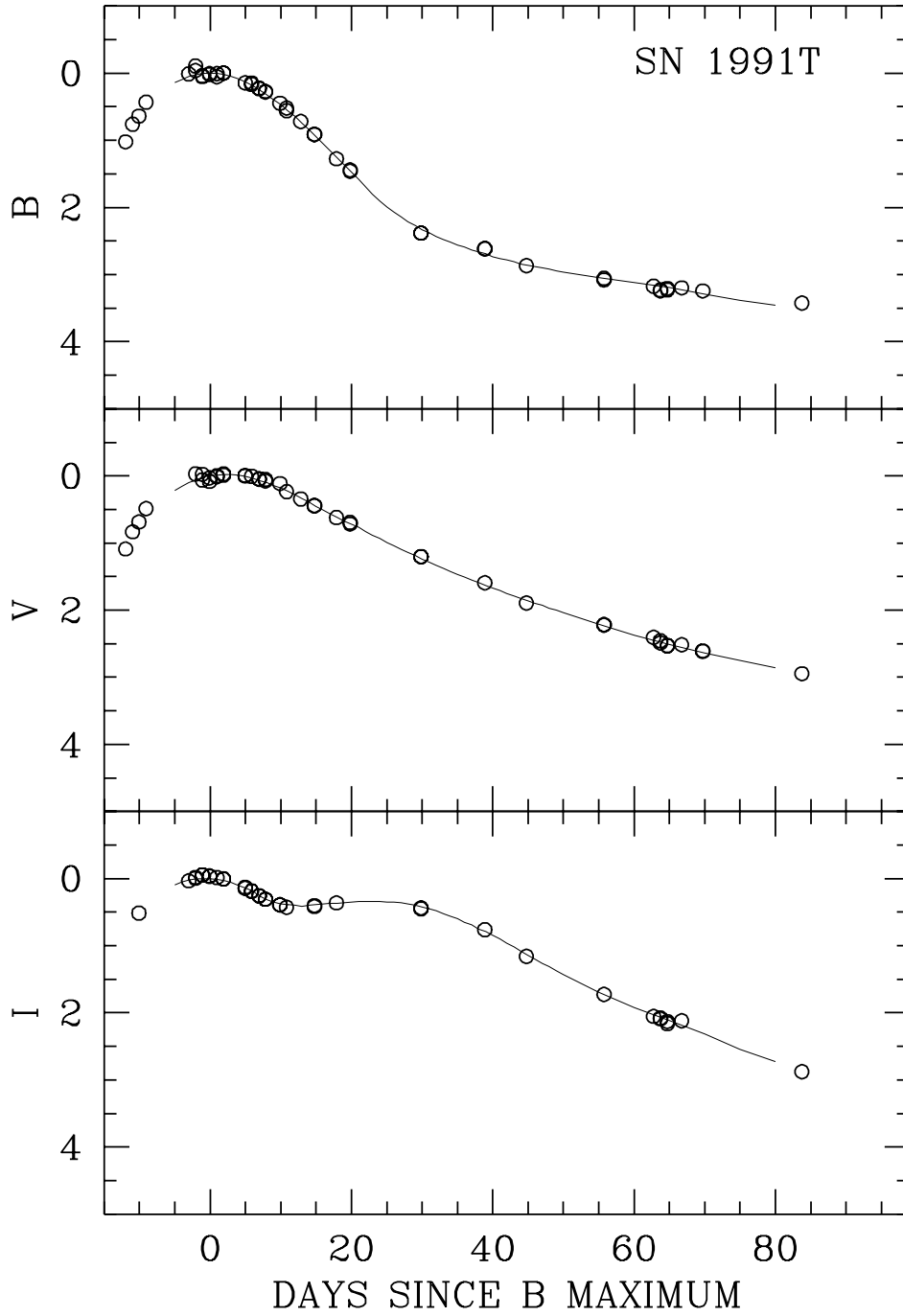


Figure 2: The B (top), V (middle), and I (bottom) light curves of SN 1991T, duly normalized, along with the calculated template. The B template is characterized by  $\Delta m_{15}(B)=0.94^m$ .

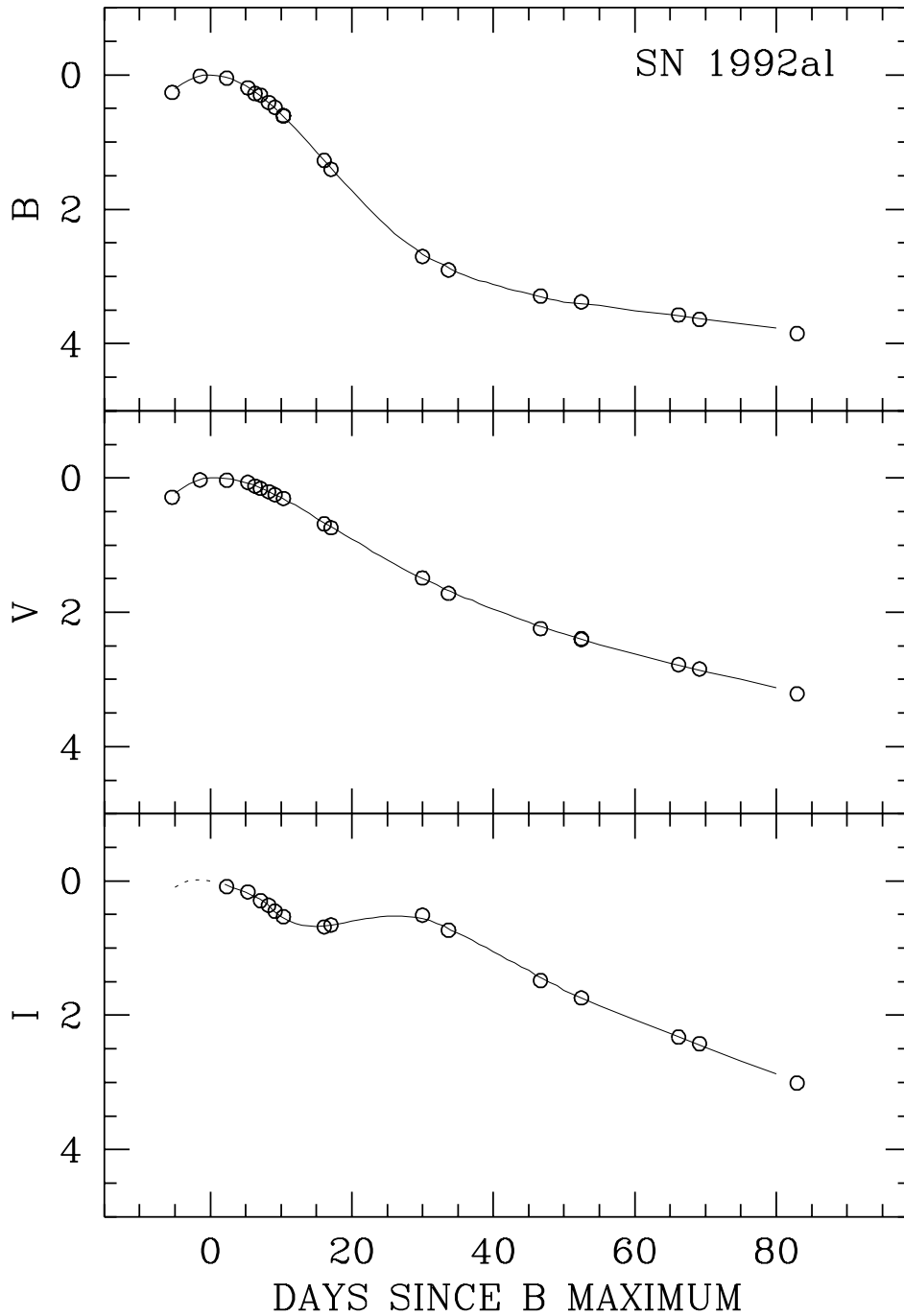


Figure 3: The B (top), V (middle), and I (bottom) light curves of SN 1992al, duly normalized and corrected for time dilation, along with the calculated template. Shown as dotted lines in the bottom panel is an extension to the calculated template I light curve, based on an average of the remaining templates. The B template is characterized by  $\Delta_{m_{15}}(B)=1.11^m$ .

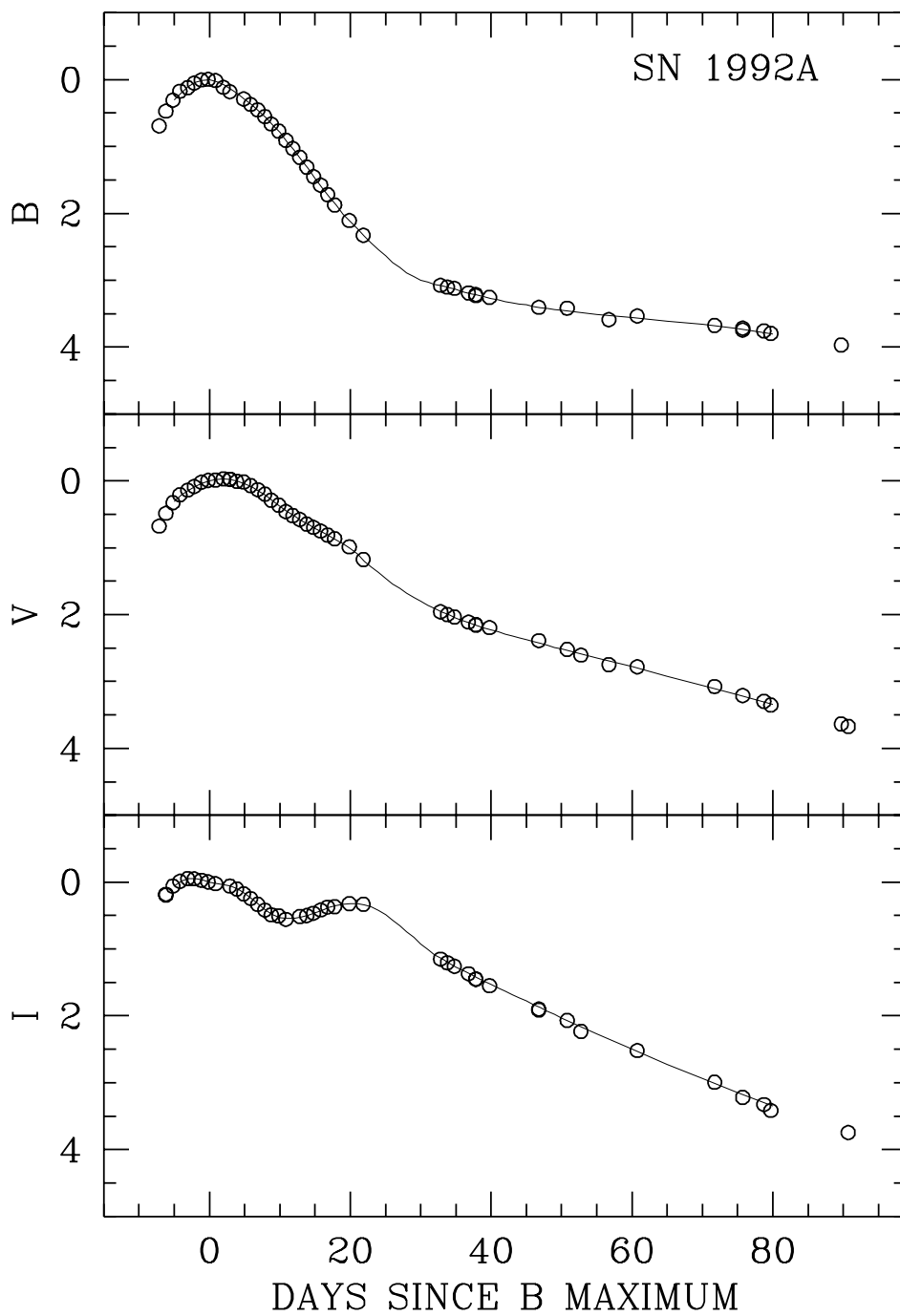


Figure 4: The B (top), V (middle), and I (bottom) light curves of SN 1992A, duly normalized, along with the calculated template. The B template is characterized by  $\Delta m_{15}(B)=1.47^m$ .

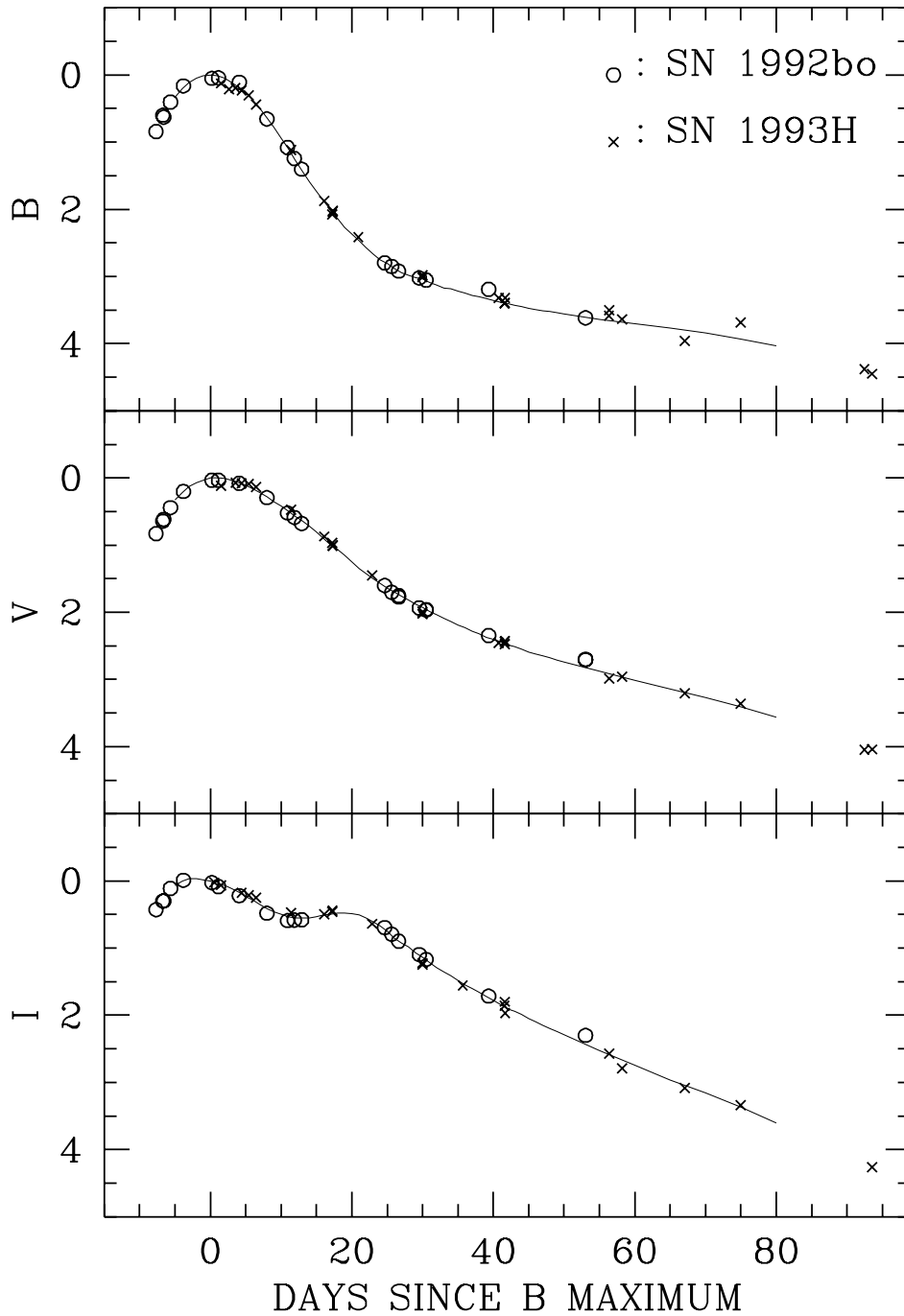


Figure 5: The B (top), V (middle), and I (bottom) light curves of SNe 1992bo (open circles) and 1993H (crosses), duly normalized and corrected for time dilation, along with the calculated template. The B template is characterized by  $\Delta m_{15}(B)=1.69^m$ .

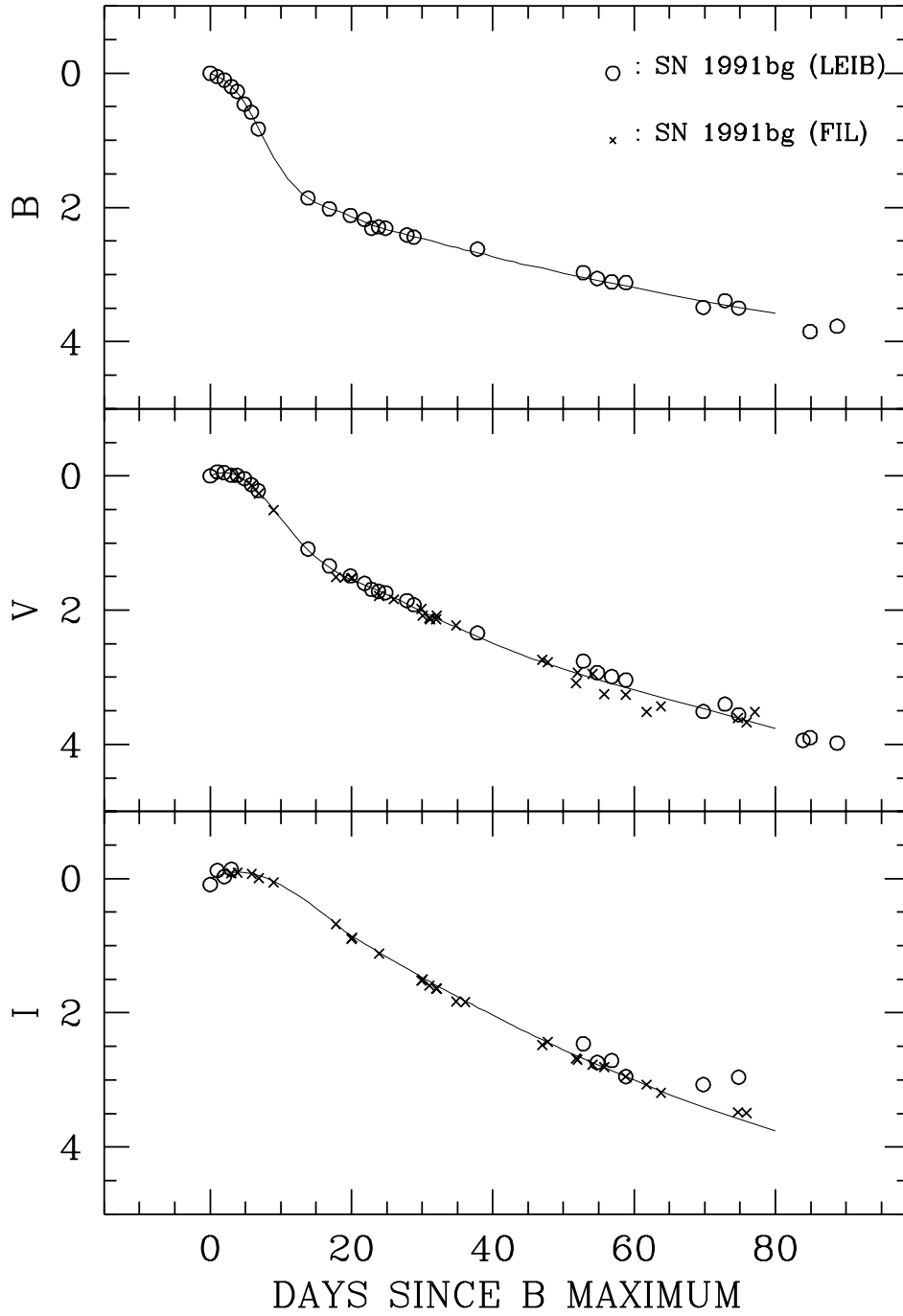


Figure 6: The B (top), V (middle), and I (bottom) light curves of SN 1991bg, duly normalized, along with the calculated template. The B template is characterized by  $\Delta m_{15}(B)=1.93^m$ .

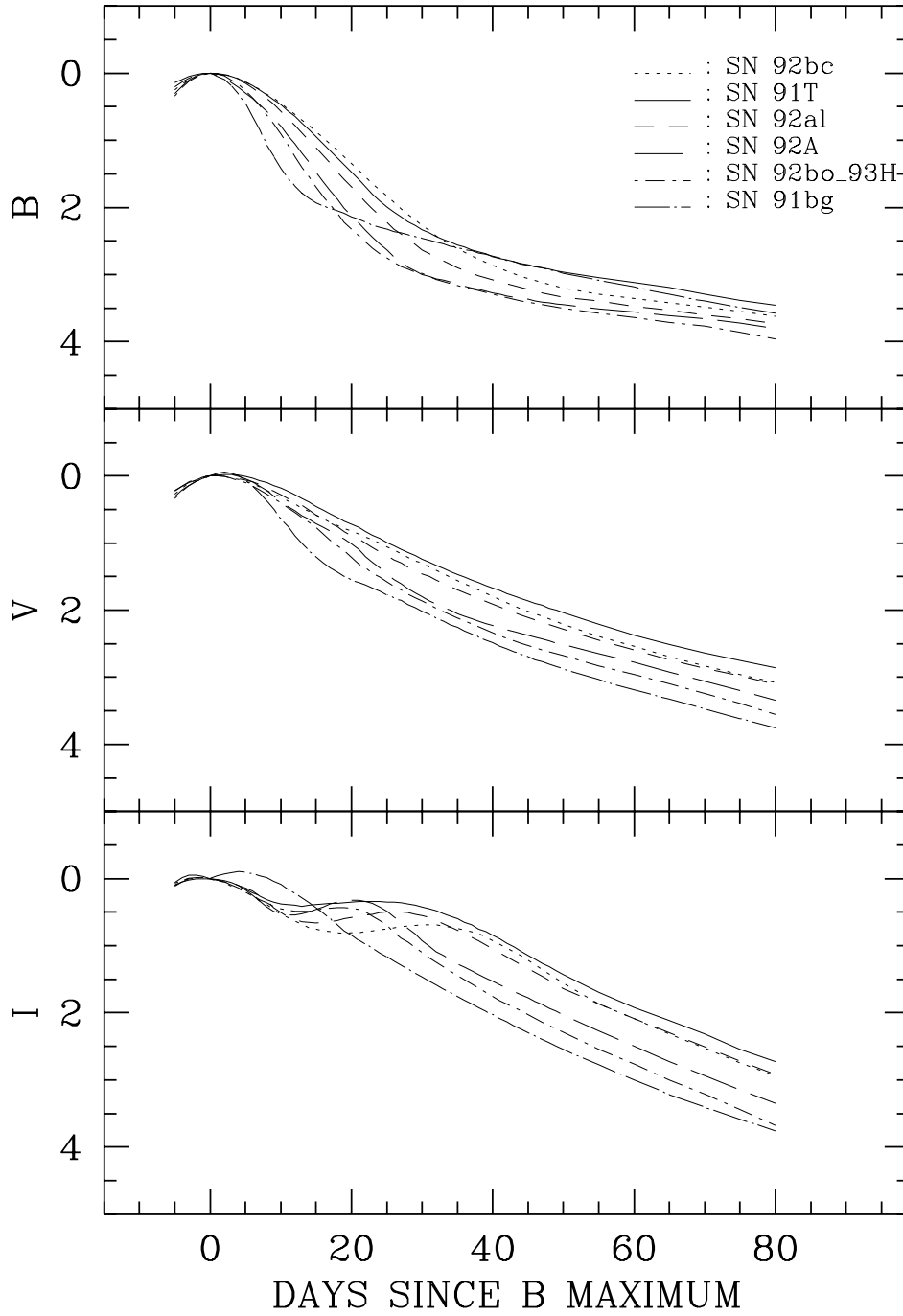


Figure 7: The comparison of the six template B (top), V (middle), and I (bottom) light curves of SNe Ia, all normalized such that  $m^k(t_0^B)=0$  in all three bands ( $k=B,V,I$ ).

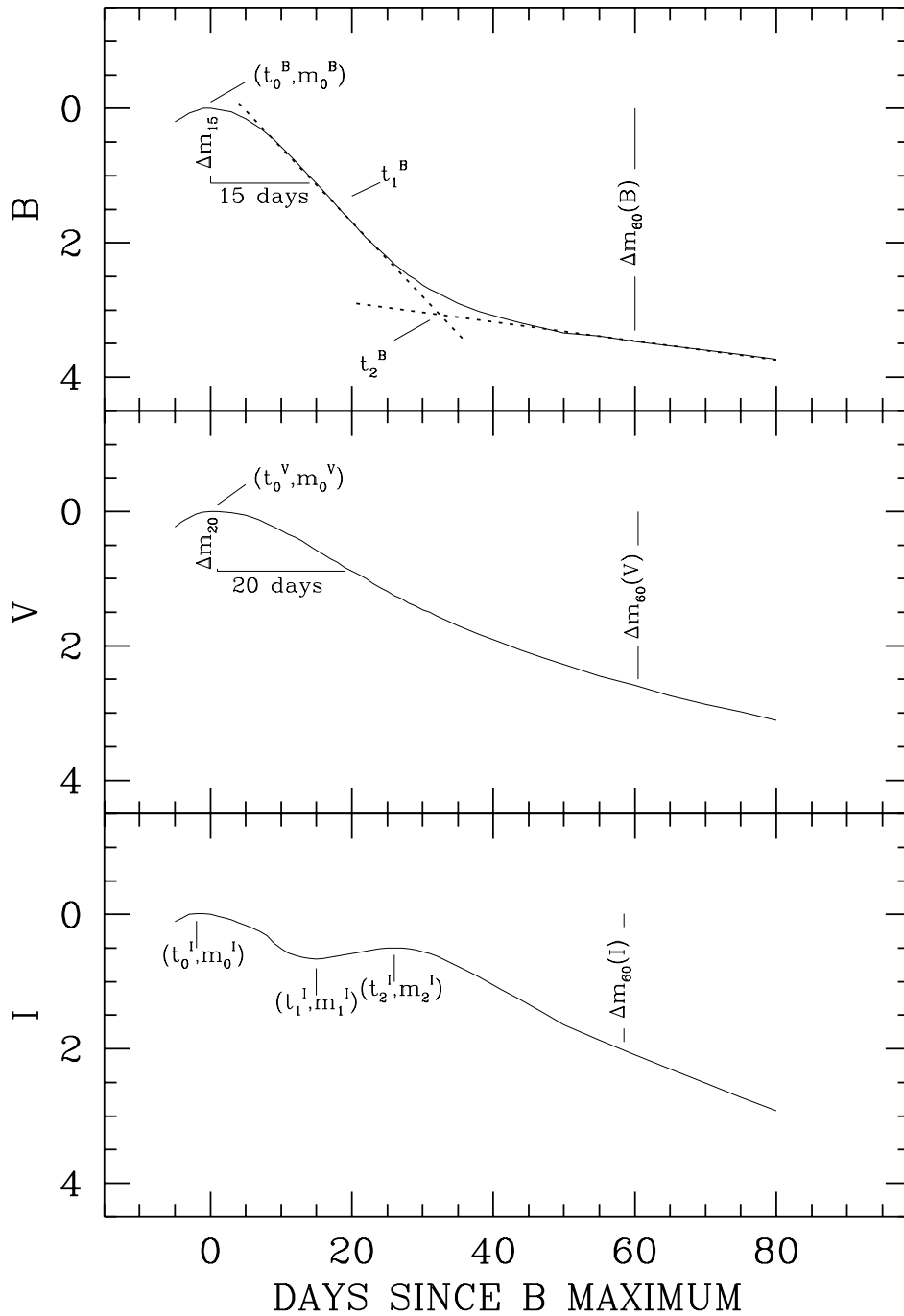


Figure 8: The template B (top), V (middle), and I (bottom) light curves of SN 1992al. Also shown are the graphical representations of the key parameters defined here in order to characterize the shape of the individual templates.

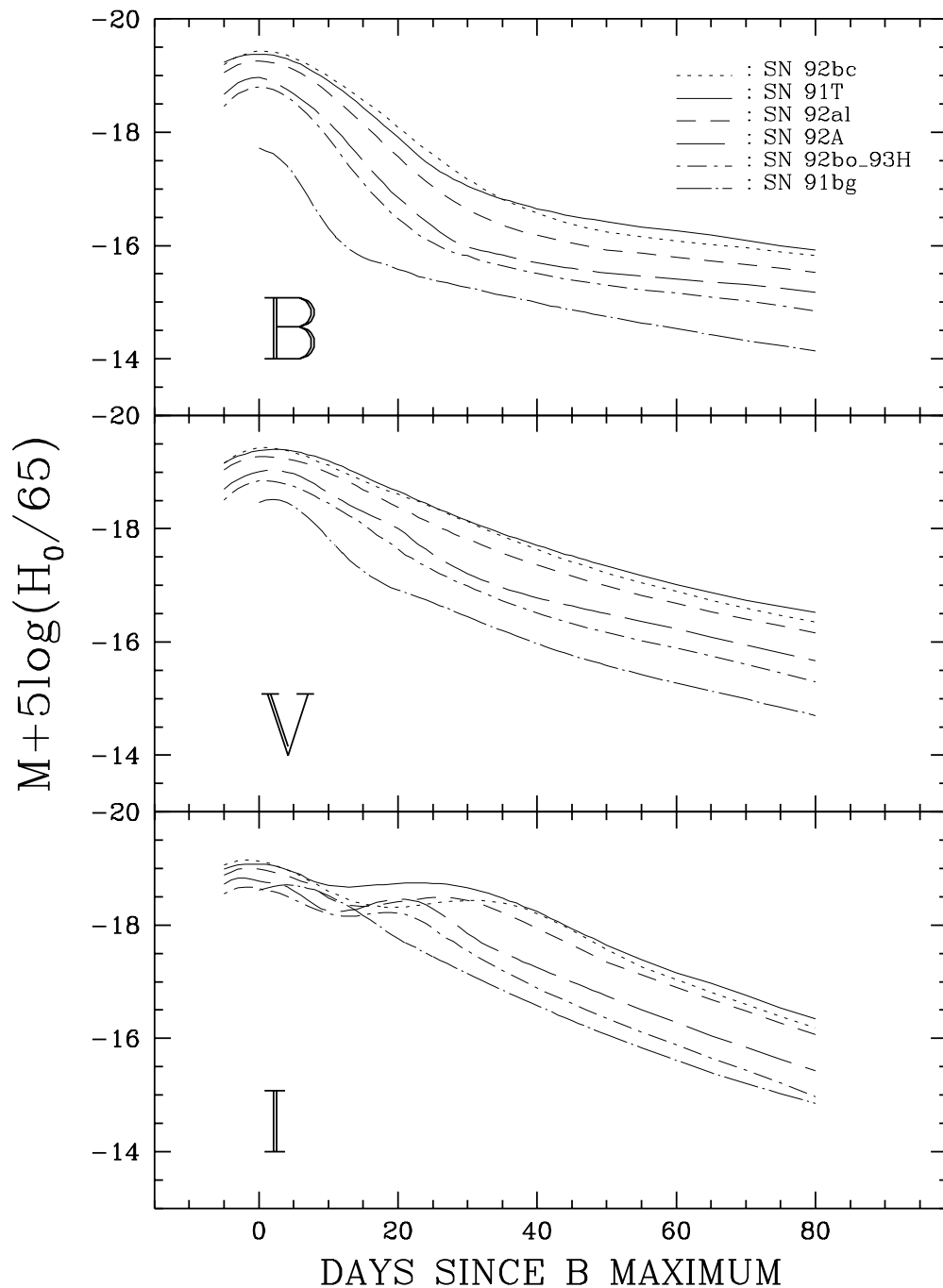


Figure 9: The six templates B (top), V (middle), and I (bottom) light curves of SNe Ia, on the absolute magnitude scale set by the peak luminosity- $\Delta m_{15}(B)$  relationship of Paper V. The peak absolute magnitudes for the five templates with  $0.87 \leq \Delta m_{15}(B) \leq 1.69$  were calculated using the “low-extinction” fits given in Table 3 of Paper V. The SN 1991bg template is plotted at the peak absolute magnitudes given in Table 1 of Paper V for the fast-declining event SN 1992K.

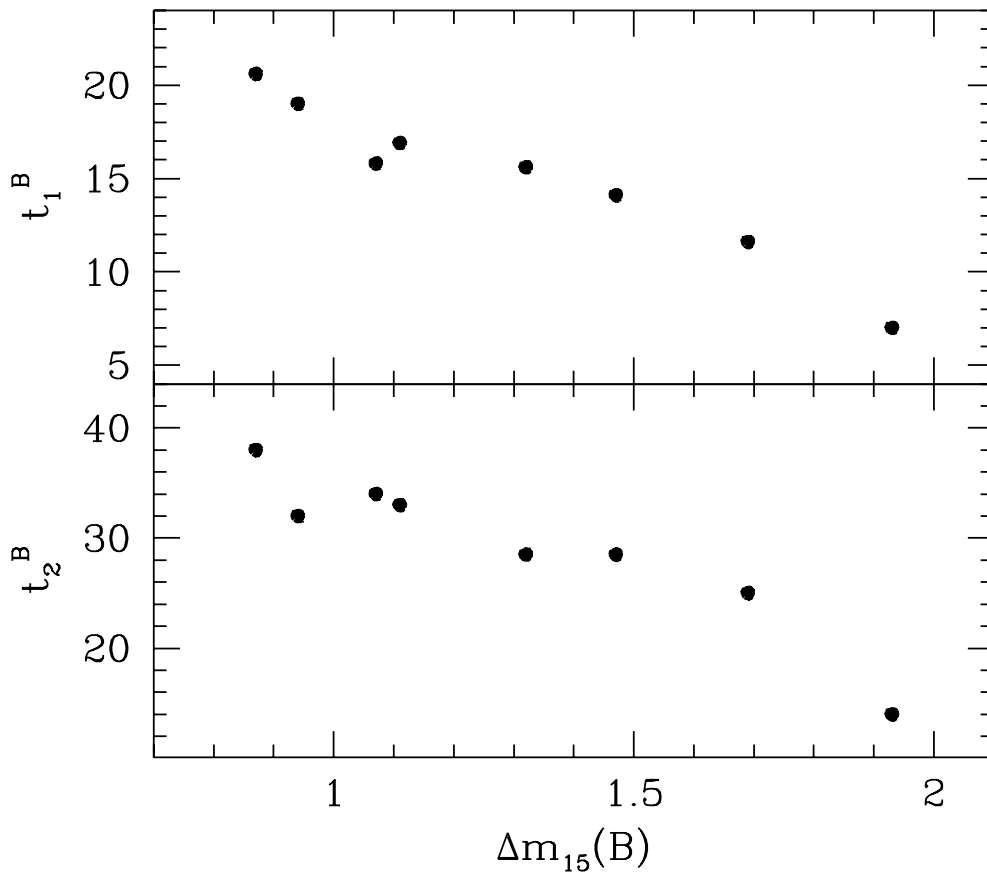


Figure 10: (top) The *inflection* point of the B light curve,  $t_1^B$ , as a function of  $\Delta m_{15}(B)$ . (bottom) The *intersection* point of the B light curve,  $t_2^B$ , as a function of  $\Delta m_{15}(B)$ .

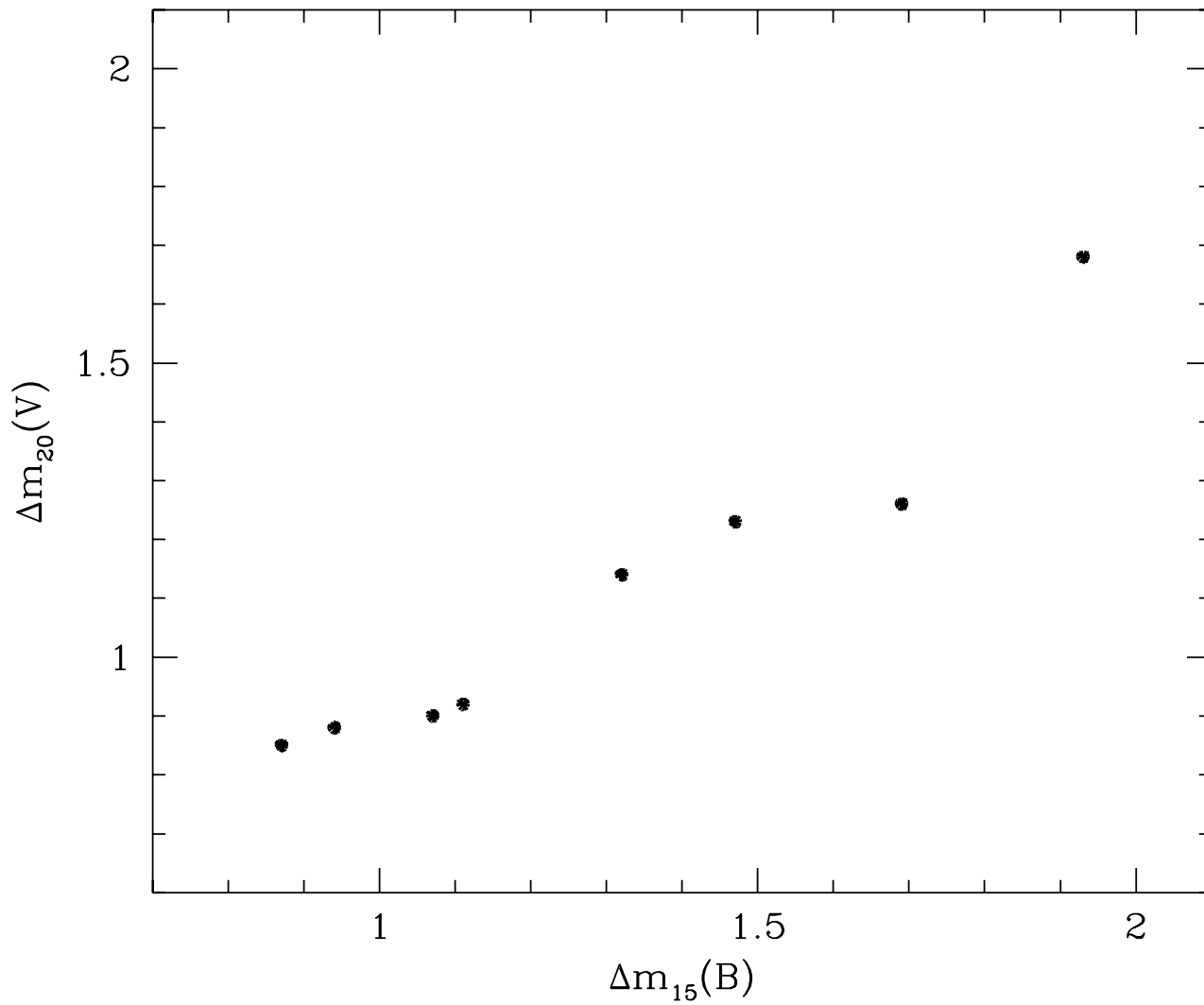


Figure 11: The initial decline rate of the V template light curves,  $\Delta m_{20}(V)$ , plotted as a function of the initial decline rate of the B template light curves,  $\Delta m_{15}(B)$ .

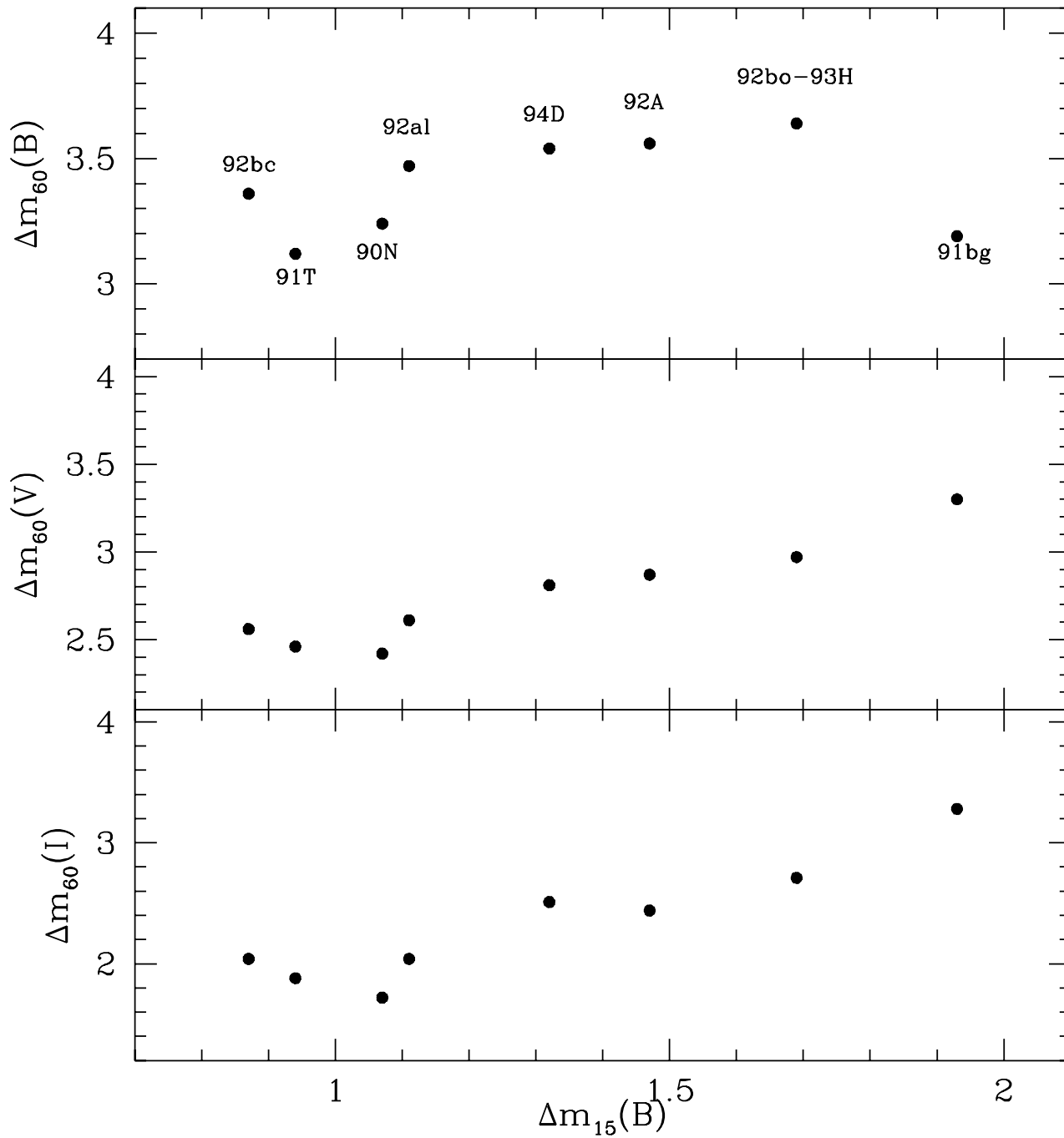


Figure 12: Comparison of the initial decline rate of the B light curve,  $\Delta m_{15}(B)$ , and the brightness of the linear tail (relative to maximum light) of the B (top), V (middle), and I (bottom) template light curves.

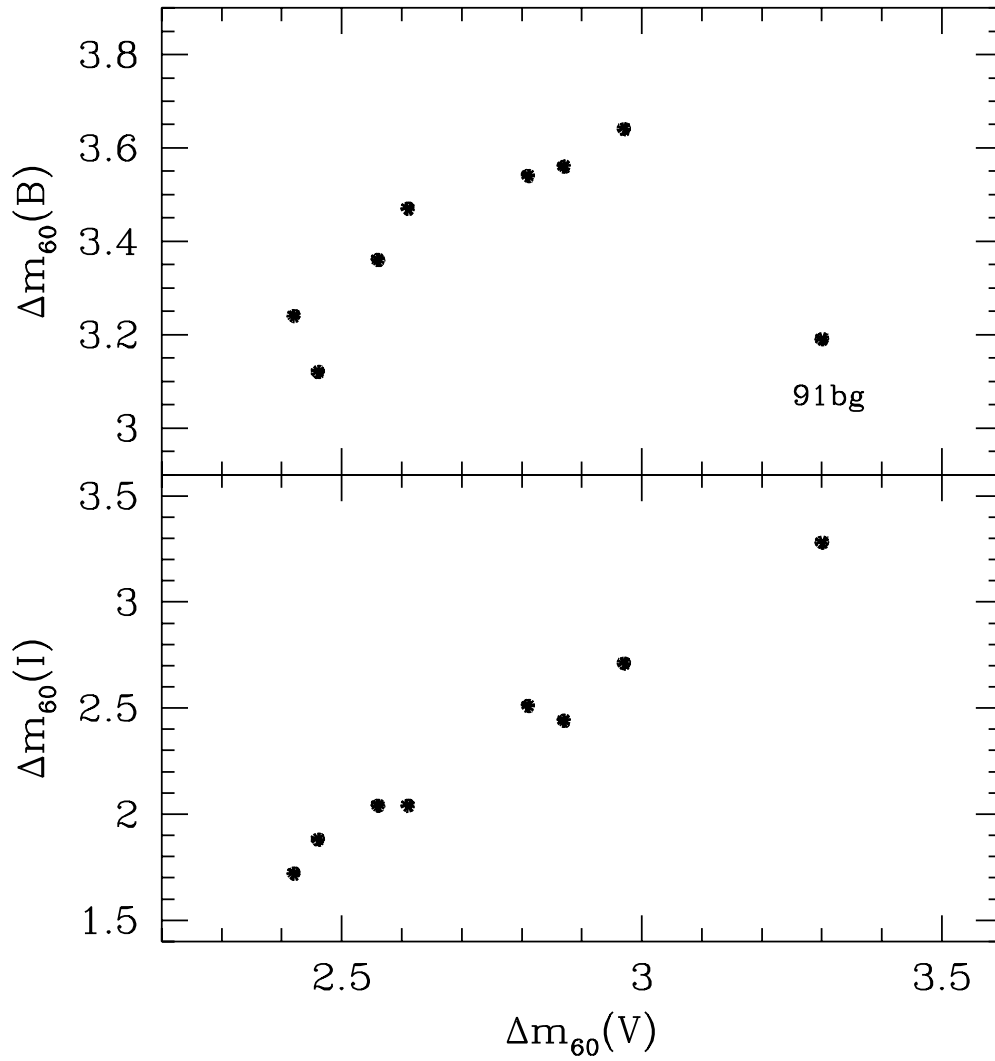


Figure 13: (top) The brightness of the linear tail (relative to maximum light) of the B template light curves, plotted as a function of the brightness of the linear tail (relative to maximum light) of the V template light curves. (bottom) The same plot for the I template curves.

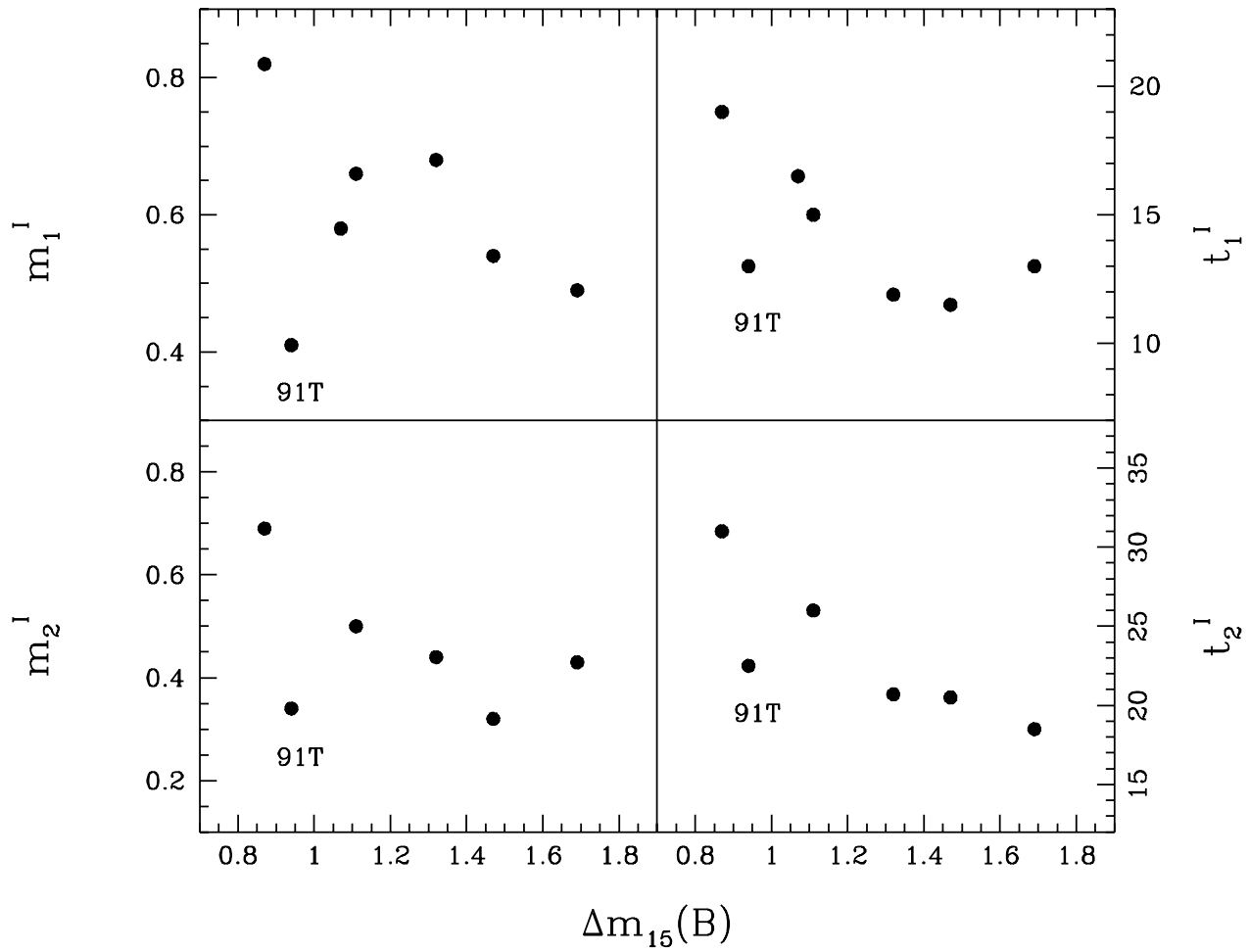


Figure 14: (top) The time and magnitude of the minimum of the I template light curves, plotted as a function of  $\Delta m_{15}(B)$ . (bottom) The time and magnitude of the secondary maximum of the I template light curves, plotted as a function of  $\Delta m_{15}(B)$ .

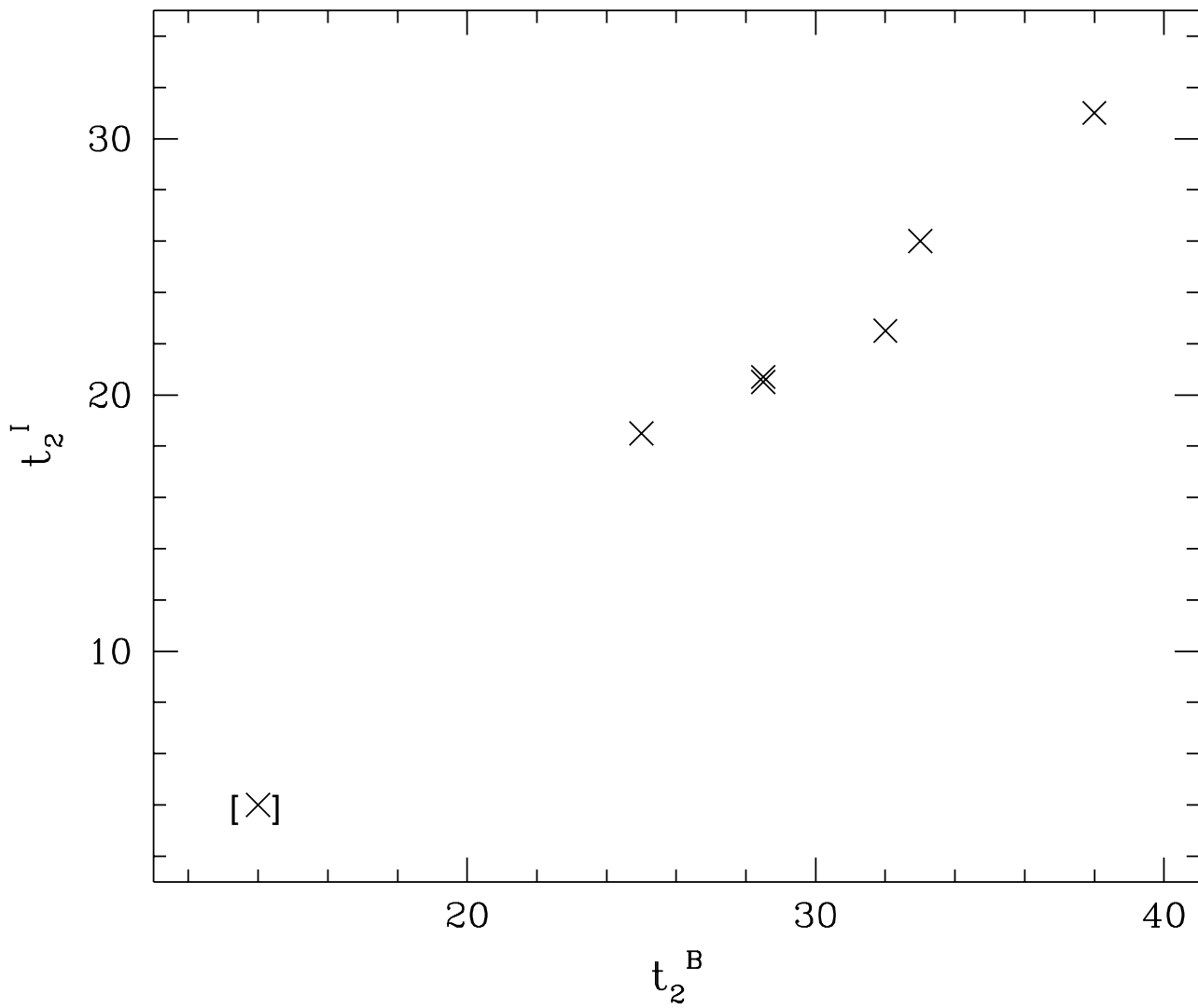


Figure 15: The time of the secondary maximum of the I template light curves,  $t_2^I$ , plotted as a function of the time of occurrence of the bend in the B light curves as measured by the *intersection* parameter,  $t_2^B$ .